JBC RESEARCH ARTICLE

The NADPH oxidase 2 subunit p47^{phox} binds to the WAVE regulatory complex and p22^{phox} in a mutually exclusive manner

Received for publication, December 22, 2023, and in revised form, February 15, 2024 Published, Papers in Press, March 1, 2024,
https://doi.org/10.1016/j.jbc.2024.107130

Simon V. N. P. Kuihon[1], Brodrick J. Sevart[1], Colette A. Abbey[2], Kayla J. Bayless[2], and Baoyu Chen[1,*]

From the [1]Roy J. Carver Department of Biochemistry, Biophysics & Molecular Biology, Iowa State University, Ames, Iowa, USA; [2]Department of Medical Physiology, Texas A&M Health Science Center, Bryan, Texas, USA

Reviewed by members of the JBC Editorial Board. Edited by Enrique De La Cruz

The actin cytoskeleton and reactive oxygen species (ROS) both play crucial roles in various cellular processes. Previous research indicated a direct interaction between two key components of these systems: the WAVE1 subunit of the WAVE regulatory complex (WRC), which promotes actin polymerization and the p47^{phox} subunit of the NADPH oxidase 2 complex (NOX2), which produces ROS. Here, using carefully characterized recombinant proteins, we find that activated p47^{phox} uses its dual Src homology 3 domains to bind to multiple regions within the WAVE1 and Abi2 subunits of the WRC, without altering WRC's activity in promoting Arp2/3-mediated actin polymerization. Notably, contrary to previous findings, p47^{phox} uses the same binding pocket to interact with both the WRC and the p22^{phox} subunit of NOX2, albeit in a mutually exclusive manner. This observation suggests that when activated, p47^{phox} may separately participate in two distinct processes: assembling into NOX2 to promote ROS production and engaging with WRC to regulate the actin cytoskeleton.

The dynamic assembly of the actin cytoskeleton and the production of reactive oxygen species (ROS) are prominently localized at membrane ruffles in actively migrating cells. The intricate interplay between these two processes is essential for a variety of biological processes, including cell adhesion, migration, phagocytosis, and tissue morphogenesis (1–8). Although extensive studies have focused on oxidative modifications of actin and various regulators of actin, including the Rho-family GTPases, the Src kinases, cofilin, myosin, gelsolin, L-plastin, and calmodulin (7, 9–12), the direct coordination between ROS-generating enzymes and actin regulators has remained elusive.

In 2003, Terada's group made a seminal observation of a direct interaction between two key regulators of these systems: the WAVE regulatory complex (WRC), which promotes actin polymerization, and the NADPH oxidase 2 complex (NOX2), which is responsible for generating ROS (13). The interaction was found to promote actin polymerization and membrane ruffling in vascular endothelial growth factor-stimulated endothelial cells (13) and play a potential role in directing the invasive migration of melanoma cells (14).

WRC is a central actin nucleation-promoting factor in the plasma membrane (15). It comprises five conserved proteins: Sra1, Nap1, Abi2, HSPC300, and the Wiskott–Aldrich syndrome family protein WAVE1 (or their corresponding mammalian orthologs in a mix-and-match arrangement). In its basal state, WRC resides in the cytosol, where it keeps WAVE1 inhibited through intramolecular interactions. WRC's activity at membranes is finely modulated through interactions with numerous membrane ligands, including inositol phospholipids, various membrane receptors bearing WRC-interacting receptor sequences, small G proteins such as Rac1 and Arf1, and various scaffolding proteins (15, 16). Activation of WRC involves the binding of Rac1 and/or Arf1 at three distinct sites, leading to the release of WAVE1's C-terminal WH2-central-acidic (WCA) domain, which in turn stimulates Arp2/3-mediated actin polymerization and lamellipodia formation in migrating cells (17–23).

NOX2 is a crucial enzyme responsible for generating ROS in various cell types (24–27). The holoenzyme of NOX2 undergoes dynamic assembly involving three cytosolic proteins (p47^{phox}, p40^{phox}, and p67^{phox}) and three membrane-associated proteins (Rac1 or Rac2, p22^{phox}, and the catalytical core gp91^{phox}) (26–29). In its resting state, gp91^{phox} remains inactive, while p47^{phox} is autoinhibited in the cytosol (30–33). The autoinhibition of p47^{phox} is achieved through its C-terminal autoinhibitory region (AIR), which obstructs the p22^{phox}-binding pocket formed between the N-terminal dual Src homology 3 (SH3) domains (31, 32). The assembly and concurrent activation of the NOX2 holoenzyme hinge upon the phosphorylation of the AIR sequence by various kinases (26). Phosphorylation dislodges the AIR sequence from the p22^{phox}-binding pocket, allowing the latter to bind to the proline-rich region (PRR) within the intracellular domain (ICD) of p22^{phox} (31, 34). This orchestrated process is essential for exerting precise spatiotemporal control over NOX2 activation and the subsequent generation of ROS (26, 35).

Terada's work indicated that the interaction between WRC and NOX2 is mediated by the PRR of WAVE1 binding to individual SH3 domains of p47^{phox} (13). Intriguingly, when a

* For correspondence: Baoyu Chen, stone@iastate.edu.
Present address for Brodrick J. Sevart: Colorado School of Mines/NREL Advanced Energy Systems Graduate Program, 1500 Illinois Street, Golden, CO 80401, USA.

mutation was introduced at the highly conserved residue, W193, within the p22^{phox}-binding pocket, it disrupted the binding to p22^{phox} but did not affect the interaction with WAVE1 (13). These data suggest that the SH3 domains of p47^{phox} use a distinct surface for binding to the PRR of WAVE1, potentially allowing a single p47^{phox} molecule to simultaneously assemble into NOX2 and interact with WRC, forming a large signalosome to coordinate ROS production and actin remodeling (13, 35).

In this study, we used carefully characterized recombinant proteins to rigorously investigate the interaction between p47^{phox} and WRC. Surprisingly, we found that the dual SH3 domains but not individual SH3 domains of p47^{phox} directly interacted with multiple sequences within the fully assembled WRC. Moreover, the interaction did not appear to impact WRC's activity in stimulating Arp2/3-mediated actin polymerization. Remarkably, we found that both WRC and p22^{phox} bound to the same pocket in p47^{phox} but they did so in a mutually exclusive manner. Therefore, our data suggest a distinct model in which activated p47^{phox} may separately participate in two crucial processes: assembling into NOX2 to stimulate ROS production and interacting with WRC to regulate the actin cytoskeleton.

Results

WAVE1 and p22^{phox} share the same binding site on p47^{phox}

Due to challenges in producing recombinant WAVE1, previous studies relied on yeast two-hybrid assays and *in vitro* translated, unpurified proteins to investigate the interaction between WAVE1 and p47^{phox} (13). To validate the previous results, we purified various fragments of p47^{phox} and the full-length (FL) WAVE1 recombinantly using established protocols (Fig. 1*A*) (36, 37). Consistent with prior findings, our pull-down assays confirmed a robust interaction between p47^{phox} and both FL WAVE1 and p22^{phox} ICD (referred to as p22^{phox} for brevity hereafter). Specifically, glutathione-*S*-transferase (GST)-tagged dual SH3 domains of p47^{phox} (hereafter referred to as p47^{phox} AB, Fig. 1*A*), but not GST, retained both maltose-binding protein (MBP)-tagged FL WAVE1 and MBP-tagged p22^{phox}, while the mutant p22^{phox}, in which the p47^{phox}-binding PRR sequence was replaced with alanines, failed to bind to p47^{phox} AB (Fig. 1*B*, lanes 1–6). Contrary to previous findings, which suggested that the W193R mutation in the p22^{phox}-binding pocket only disrupted the binding to p22^{phox} but not to WAVE1 (13), it was to our surprise that W193R abolished the binding to both p22^{phox} and FL WAVE1 (Fig. 1*B*, lanes 7–9). This result indicated that, distinct from the previous conclusions, WAVE1 and p22^{phox} may share the same binding pocket on p47^{phox}.

To further investigate the previous model which proposed that WAVE1 and p22^{phox} can simultaneously bind to the same p47^{phox} (13), we used two distinct approaches. First, in a competition pull-down assay, we observed that the WT p22^{phox} ICD peptide, but not the mutant peptide, significantly suppressed the binding to WAVE1 (Fig. 1*C*). Next, we used a far pull-down assay to test whether untagged p47^{phox} AB could act as a bridge between p22^{phox} and WAVE1, which would support the idea of their simultaneous binding to the same

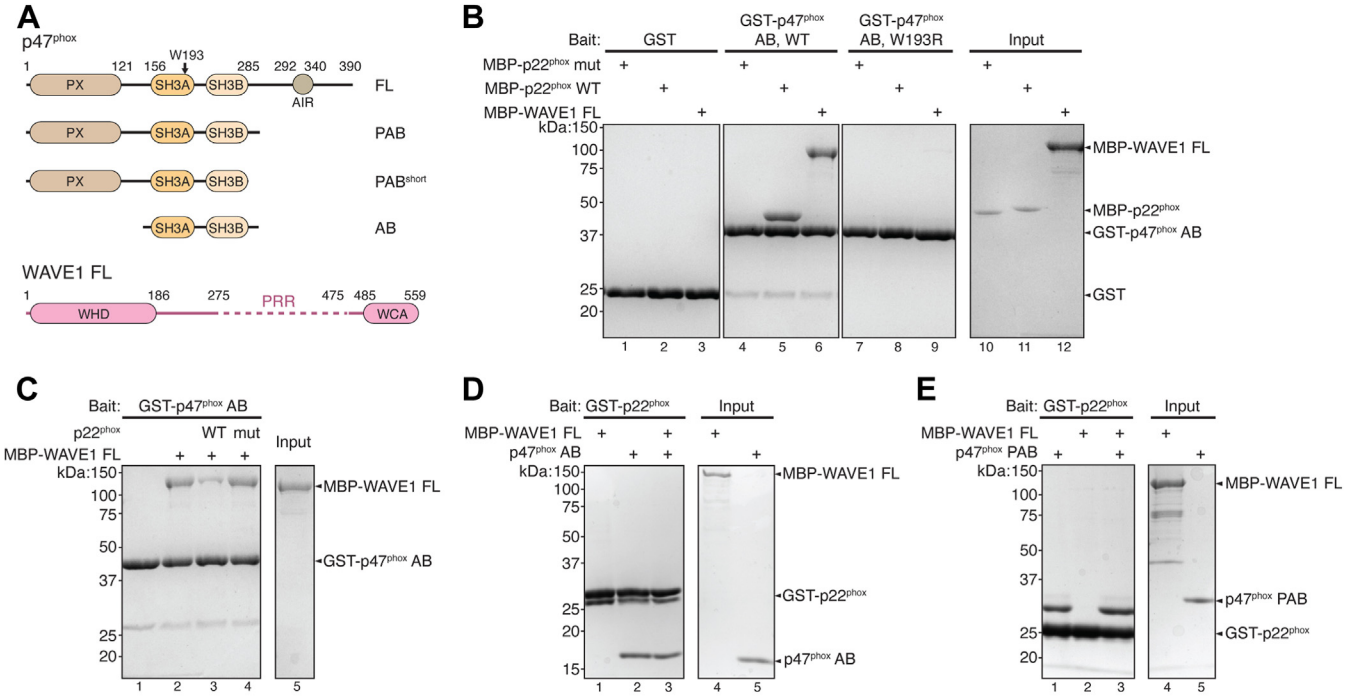

Figure 1. p47^{phox} binds to full-length WAVE1. *A*, schematic showing domain organization and constructs used in this study. *B–E*, *Coomassie blue–stained* SDS PAGE gels showing glutathione-*S*-transferaseGST) pull-down between GST-p47^{phox} AB or GST-p22^{phox} and FL WAVE1 in indicated conditions. *B*, WT and W193R mutant of GST-p47^{phox} AB pulling down MBP-p22^{phox} and MBP-FL WAVE1. *C*, GST-p47^{phox} AB pulling down FL WAVE1 in the presence of p22^{phox} ICD peptide as competitors. *D* and *E*, far pull-down results of FL WAVE1 by GST-p22^{phox} in the presence of untagged p47^{phox} AB in (*D*) or PAB in (*E*). ICD, intracellular domain; MBP, maltose-binding protein.

p47^{phox}. However, our experiments failed to detect any interaction between GST-p22^{phox} and FL WAVE1 in the presence of untagged p47^{phox}, whether it is the AB construct or the longer PAB construct (where P stands for the phox-homology or PX domain) (Fig. 1, *A*, *D*, and *E*). Together, our data strongly indicate that the interactions of both WAVE1 and p22^{phox} with p47^{phox} occur through the same binding pocket and are mutually exclusive.

WRC interacts with p47^{phox} at the same binding pocket

Inside the cell, WAVE1 does not exist as a single polypeptide chain but instead is constitutively incorporated into the WRC (Fig. 2*A*) (15). As a result of the limited availability of WRC purification techniques, earlier studies relied on isolated WAVE1 to explore its interaction with p47phox (13). Over the last 2 decades of efforts to refine WRC purification methods, it has become evident that isolated WAVE1 has a tendency to aggregate, potentially introducing experimental artifacts (15, 36, 38). To investigate whether the interaction between p47^{phox} and FL WAVE1 holds true in the context of the WRC, we used recombinantly purified FL WRC in pull-down assays. Surprisingly, in contrast to previous findings, only tandemly linked dual SH3 domains (*i.e.*, GST-p47^{phox} AB), and not the individual A or B SH3 domains, were able to bind the WRC (Fig. 2*B*, lanes 9–11). This is similar to p22^{phox}, which also required both SH3 domains but not individual ones for binding (Fig. 2*B*, lanes 2–4). The N-terminal PX domain slightly weakened the binding to p22^{phox} but did not seem to affect the binding to WRC (Fig. 2*B*, lanes 5 and 12).

It is well-established that the FL p47^{phox} protein is autoinhibited due to its AIR sequence binding to the p22^{phox}-binding pocket, which prevents p22^{phox} from binding (Fig. 2*A*) (31, 32). Consistent with this concept, our experiments showed that the purified FL p47^{phox} did not bind to either WRC or p22^{phox}. In contrast, when we mutated the AIR region to release the autoinhibition, the binding to both WRC and p22^{phox} was restored (Fig. 2*B*, lanes 6–7, 13–14). Furthermore, the interaction between FL WRC and p47^{phox} was effectively blocked by the addition the WT p22^{phox} peptide, while the mutant peptide had no such effect (Fig. 2*C*). Moreover, the interaction was abolished by the W193R mutation in the p22^{phox}-binding pocket of p47^{phox} (Fig. 2*D*). In summary, these data confirm that WRC and p22^{phox} compete for the same pocket in p47^{phox}.

p47^{phox} interacts with the WAVE1–Abi2–HSPC300 subcomplex

To dissect the regions mediating the interaction between FL WRC and p47^{phox}, we tested which subcomplexes of the WRC

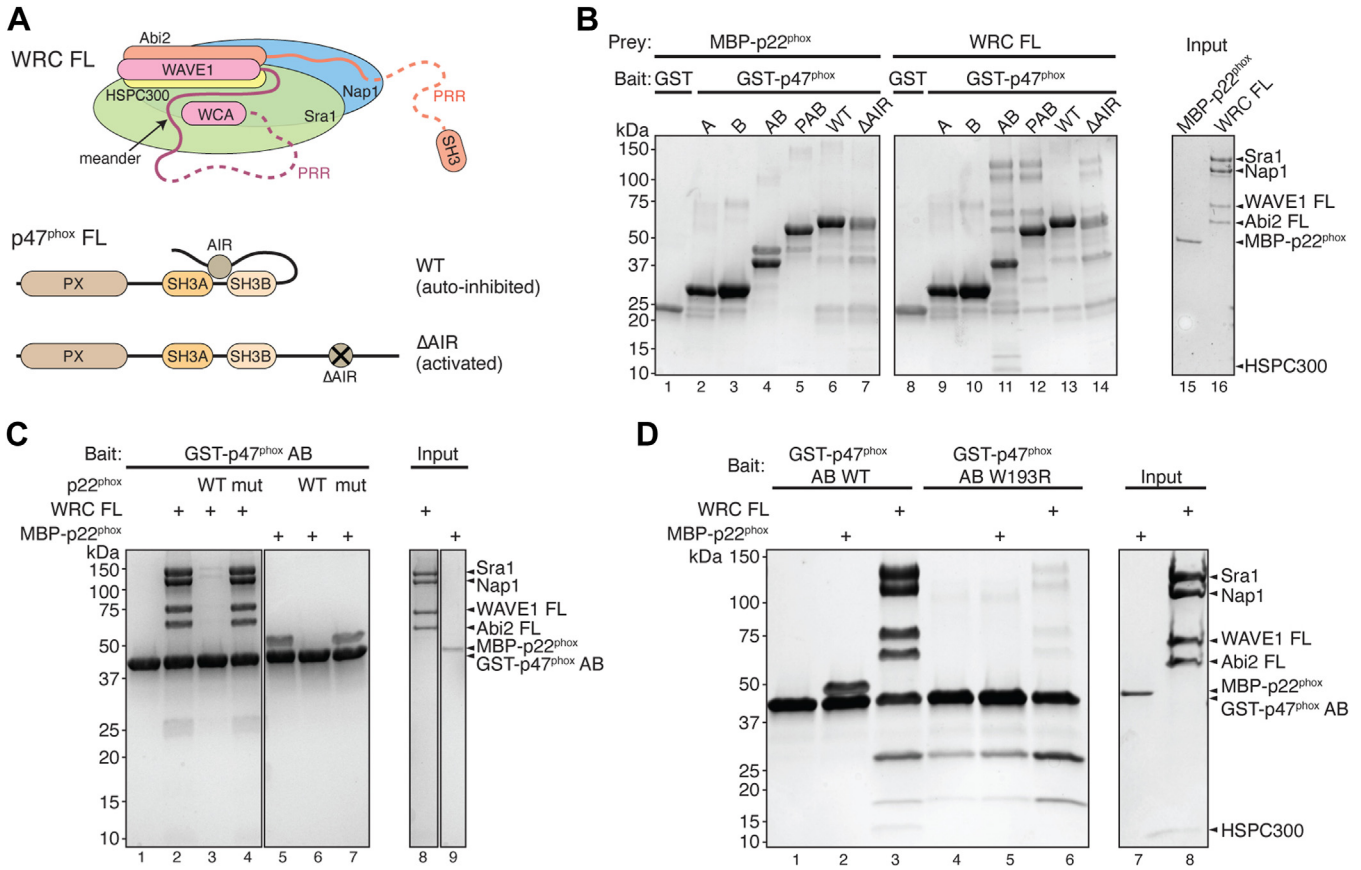

Figure 2. p47^{phox} binds to full-length WRC. *A*, schematic showing WRC structure and domain organization used in this study. *B–D*, *Coomassie blue–stained* SDS-PAGE gels showing glutathione-*S*-transferase (GST) pull-down results. *B*, different GST-p47^{phox} truncations pulling down MBP-p22^{phox} and FL WRC. *C*, GST-p47^{phox} AB pulling down FL WRC in the presence of p22^{phox} ICD peptide as competitors. *D*, pull-down of FL WRC by WT or mutant GST-p47^{phox} AB. ICD, intracellular domain; MBP, maltose-binding protein; WRC, WAVE regulatory complex.

could bind to GST-p47^{phox} AB. In previous studies, isolated subunits of WRC often encountered issues with protein aggregation, which led to artificial results (15). However, two partially assembled subcomplexes were found to be relatively stable and suitable for biochemical studies, including a dimer containing Sra1 and Nap1, and a trimer containing WAVE1, Abi2, and HSPC300 (Fig. 3*A*) (36, 38).

We found that GST-p47^{phox} AB robustly pulled down an MBP-tagged WAVE1-Abi2-HSPC300 trimer but it did not interact with the Sra1-Nap1 dimer (Fig. 3*B*). Similar to the interaction between WRC and p47^{phox}, this interaction was effectively blocked by the WT p22^{phox} peptide, but not by the mutant peptide (Fig. 3*C*). Based on these results, we conclude that the interaction between WRC and p47^{phox} is mediated by the WAVE1-Abi2-HSPC300 portion of the WRC.

p47^{phox} binds to multiple regions in WAVE1 and Abi2

In the trimer, both WAVE1 and Abi2 possess long unstructured sequences. Unlike their N-terminal helices, these C-terminal unstructured sequences are not involved in assembling the WRC or the WAVE1–Abi2–HSPC300 subcomplex and contain various PRR sequences, which may be important for binding to proteins containing SH3 or EVH1 domains (15, 16, 37, 39). To further identify the regions responsible for binding to p47^{phox}, we generated trimers in which the PRR sequences in either WAVE1 or Abi2 were removed (Fig. 4*A*). We found that the unstructured regions of either WAVE1 or Abi2 were sufficient to sustain the interaction with p47^{phox} AB, and this interaction could be efficiently blocked by p22^{phox} ICD peptide (Fig. 4*B*). This result suggests that p47^{phox} AB binds to both WAVE1 and Abi2.

To narrow down the regions within the unstructured sequences responsible for this interaction, we divided the unstructured regions in WAVE1 and Abi2 into shorter fragments, each of ∼60 residues in length and assessed their individual interactions with p47^{phox} (Fig. 4, *B* and *C*). We found that in WAVE1, fragment #4 (residues 419–480) clearly exhibited an interaction with p47^{phox} (Fig. 4*B*, lane 12, asterisk). This result aligns with previous report, in which WAVE1 (residues 270–442) was found to be important for WAVE1 to bind to p47^{phox} (13). In Abi2, fragment #1 (residues 162–238) and, to a lesser extent, fragment #2 (residues 239–319) displayed interactions with p47^{phox} (Fig. 4*C*, lanes 2–3, asterisks). Together, we conclude that p47^{phox} can bind to at least three distinct PRR regions in the unstructured sequences of WAVE1 and Abi2. Note that the binding affinity of

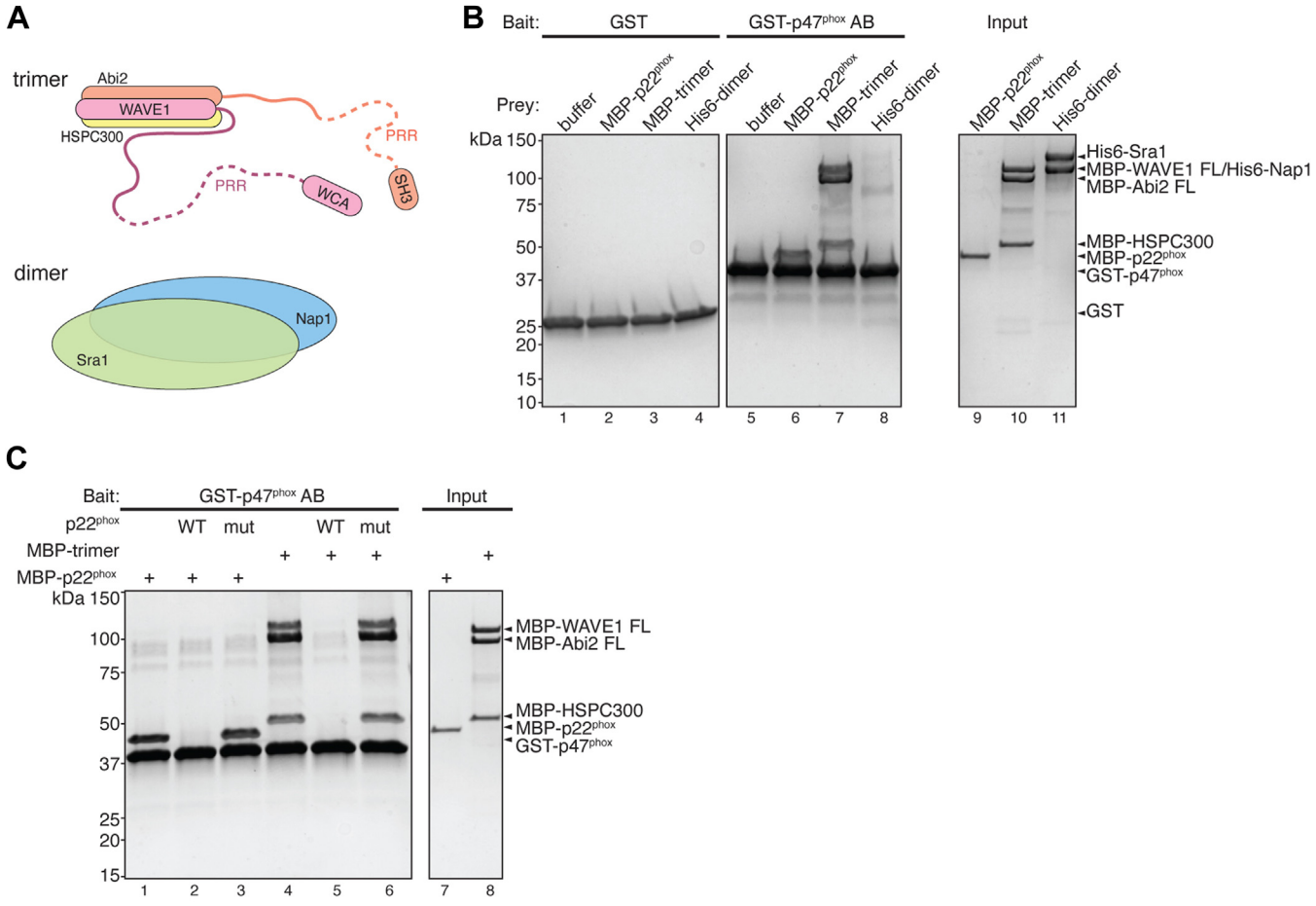

Figure 3. p47^{phox} binds to WAVE1–Abi2–HSPC300 subcomplex of WRC. *A*, schematic showing WRC subcomplexes used in this study. *B* and *C*, *Coomassie blue–stained* SDS-PAGE gels showing glutathione-*S*-transferase (GST) pull-down results. *B*, GST-p47^{phox} AB pulling down WRC indicated subcomplexes. *C*, GST-p47^{phox} AB pulling down trimer in the presence of p22^{phox} ICD peptide as competitors. ICD, intracellular domain; WRC, WAVE regulatory complex.

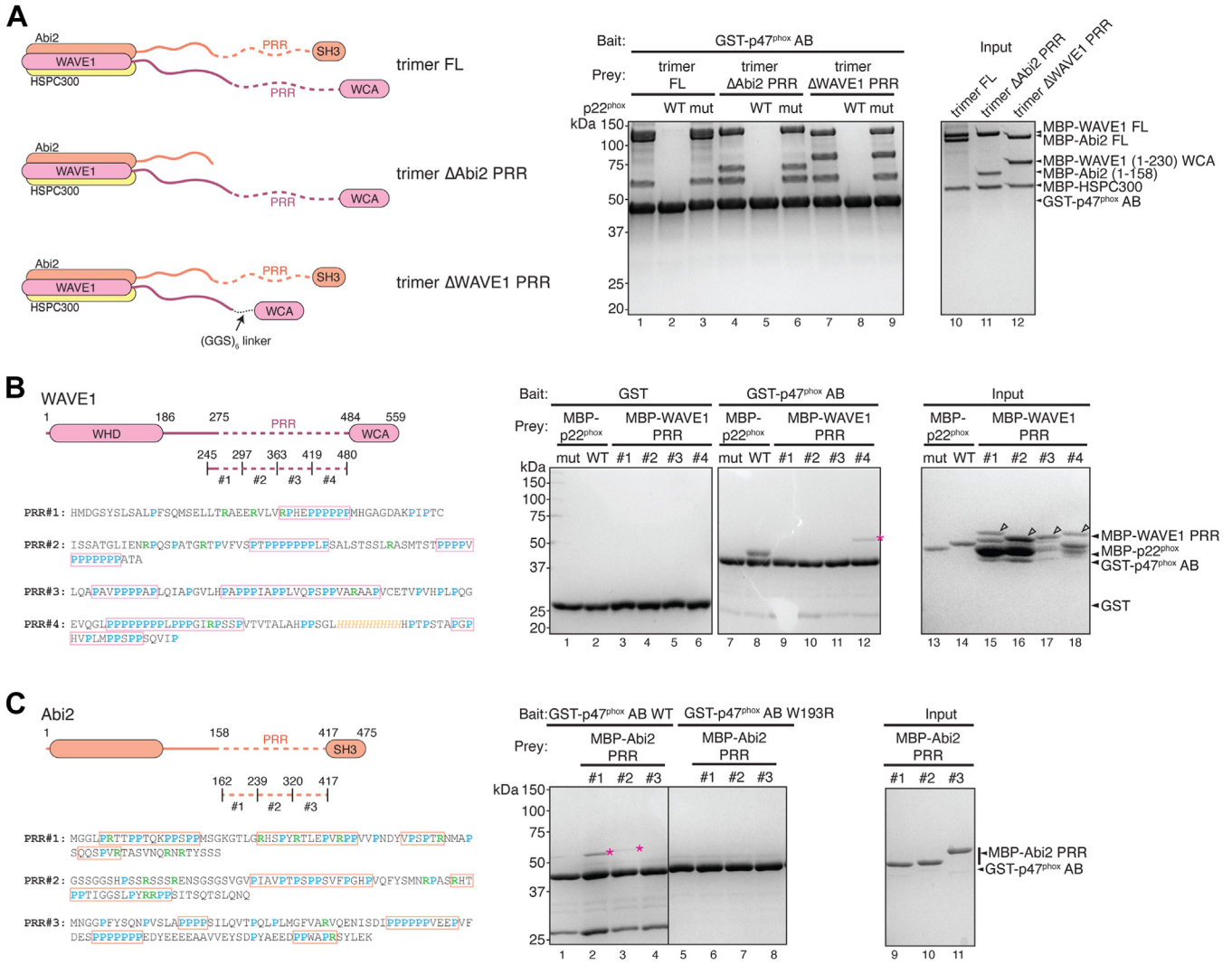

Figure 4. p47^{phox} binds to multiple PRR sequences in WAVE1 and Abi2. Schematic and *Coomassie blue–stained* SDS-PAGE gels showing glutathione-*S*-transferase (GST)-p47^{phox} AB pull down of (*A*) indicated trimers, (*B*) MBP-tagged PRR fragments of WAVE1, and (*C*) MBP-tagged PRR fragments of Abi2. In protein sequences, prolines are presented in *cyan* and arginines in *green*. PRR sequences are *boxed* based on proline density and their alignment with predicted SH3-binding sequences (40). *Arrowheads* in (*B*) indicate full-length fragments. *Magenta asterisks* indicate binding signals of corresponding fragments. MBP, maltose-binding protein; PRR, proline-rich region; SH3, Src homology 3.

individual fragments appeared to be weaker than that of the FL proteins. This suggests that other fragments may also contribute to the overall interaction observed in the context of the FL proteins, but their individual affinities were too weak to be detected using pull-down assays. It is not uncommon for the combined contributions of multiple weak-affinity regions to contribute to a strong binding observed with FL proteins, often due to avidity or cooperativity effects.

WAVE1 contains an additional, noncanonical p47^{phox} binding sequence

Based on our above results, we initially predicted that removing the unstructured regions from both WAVE1 and Abi2 would eliminate the binding of the WRC to p47^{phox}. This WRC, referred to as WRC$^{\Delta 230}$ in previous structural studies, consists of WAVE1 1 to 230 and Abi2 1 to 158, excluding the unstructured sequences at the C terminus (Fig. 5*A*) (17, 36). To our surprise, we found that WRC$^{\Delta 230}$ still exhibited robust binding to p47^{phox}. Similar to the interactions with p22^{phox} and FL WRC, the binding of WRC$^{\Delta 230}$ to p47^{phox} was abolished by the W193R mutation (Fig. 5*B*) and was competitively disrupted by the p22^{phox} peptide (Fig. 5*C*). Moreover, this binding relied on the dual SH3 domains in the activated p47^{phox}. Individual SH3 domains or the FL autoinhibited p47^{phox} did not support the interaction (Fig. 5*D*).

Note that the p47^{phox} PAB construct appeared to lose the binding to WRC$^{\Delta 230}$ (Fig. 5*D*, lane 5), although it maintained the binding to FL WRC (Fig. 2*B*, lane 12). We suspected that either the PX domain at the N terminus of the dual SH3 domains or the additional amino acid linker at the C terminus interfered with the binding to WRC$^{\Delta 230}$. To investigate this, we removed the extra amino acids at the C terminus and found that the resulting p47^{phox} PAB^{short} construct (Fig. 1*A*) exhibited an improved binding to WRC$^{\Delta 230}$ (Fig. 5*E*, lane 3). Note that the binding affinity was still weaker than p47^{phox} AB

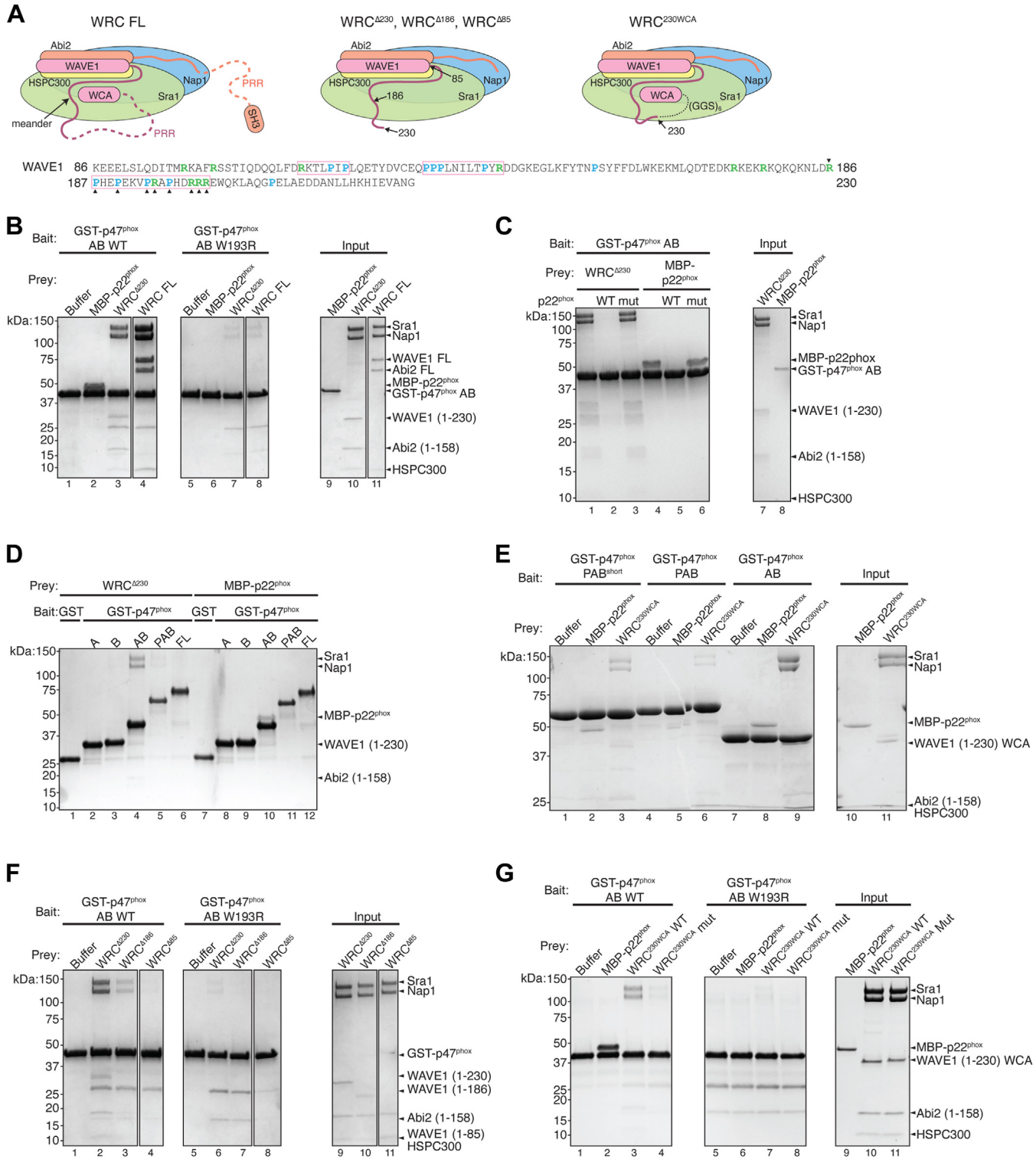

Figure 5. p47^{phox} binds to noncanonical sequences in WAVE1 86 to 230. *A*, schematic showing various WRC assemblies. WAVE1 86 to 230 sequences are shown in which prolines are presented in *cyan* and arginines in *green*, and PRR sequences are *boxed* based on proline density and their alignment with predicted noncanonical SH3-binding sequences (40). *Arrowheads* indicate residues mutated in WAVE1^{230WCA} mutant used in (*G*). *B–F*, *Coomassie blue–stained* SDS-PAGE gels showing glutathione-*S*-transferase (GST) pull-down results. *B*, shows GST-p47^{phox} AB pulling down WRC$^{\Delta230}$. *C*, GST-p47^{phox} AB pulling down WRC$^{\Delta230}$ in the presence of p22^{phox} ICD peptide as competitors. Note that the control lanes 4 to 6 are identical to lanes 5 to 7 in Figure 2*C*. *D*, pull-down results of WRC$^{\Delta230}$ by various GST-p47^{phox} constructs. *E*, pull-down results of WRC^{230WCA} comparing various GST-p47^{phox} constructs. *F*, shows GST-p47^{phox} AB pulling down indicated WRCs. *G*, shows GST-p47^{phox} AB pulling down WRC^{230WCA} WT and mutant. ICD, intracellular domain; PRR, proline-rich region; SH3, Src homology 3; WCA, WH2-central-acidic; WRC, WAVE regulatory complex.

(Fig. 5*E*, lane 9), suggesting that the PX domain might pose certain steric clashes with the bound WRC. Due to its higher binding affinity, we switched to $p47^{phox}$ PAB^{short} for experiments described hereafter that involved PAB.

We suspected that the binding between $WRC^{\Delta230}$ and $p47^{phox}$ was mediated by residues 186 to 230 in WAVE1. This region is important for WRC activation but is believed to be a flexible sequence because it remained unresolved in previous X-ray crystallography and cryo-EM studies (17, 20, 22). Consistent with our prediction, the further removal of residues 187 to 230, as in $WRC^{\Delta186}$, substantially reduced the interaction (Fig. 5*F*, lanes 2–3). Note that $WRC^{\Delta186}$ still exhibited weak residual binding to $p47^{phox}$, which was abolished by further removal of residues 86 to 186 from WAVE1, as in $WRC^{\Delta85}$ (Fig. 5*F*, lanes 3–4). Together, these data suggest that, in addition to the PRR sequences in WAVE1 and Abi2, WAVE1 86 to 230 also interacts with $p47^{phox}$ through the same $p22^{phox}$-binding pocket (Fig. 5*F*, lanes 6–8).

WAVE1 86 to 230 is not considered as a PRR and does not contain canonical SH3-binding sequences, yet it is scattered with several prolines and arginines, which are often found in SH3-binding motifs (40). To validate the importance of these residues in mediating the interaction, we mutated R186, P187, P190, P194, R195, P197, R200, R201, and R202 in $WAVE1^{\Delta230WCA}$ to alanines (Fig. 5*A*, arrowheads). As a result, the interaction was greatly reduced (Fig. 5*G*, lanes 3–4), confirming that WAVE1 186 to 230 contains noncanonical SH3-binding sequences capable of binding to $p47^{phox}$ dual SH3 domains. Note that we used WRC^{230WCA} for these experiments, as it contains the WCA domain, allowing us to measure whether this interaction influences WRC activity in the next section.

$p47^{phox}$ binding does not impact WRC activity

WAVE1 86 to 230 harbors the meander sequence known to be critical for WRC autoinhibition and activation (Fig. 5*A*), whereas the C-terminal unstructured PRR sequences do not contribute to WRC assembly or activation but allow the WRC to interact with various regulatory proteins (15, 16). Given that $p47^{phox}$ dual SH3 domains directly interacted with the WAVE1 86 to 230 sequence, we speculated that this interaction might influence WRC activity. To test this hypothesis, we used the established pyrene-actin polymerization assay to examine the effect of $p47^{phox}$ on WRC activity. Before we conducted this assay, we confirmed that the interaction observed in GST pull-down assays similarly occurred in cogel filtration chromatography (Fig. 6*A*) and when we swapped bait and prey using MBP-tagged WRC to pull down untagged $p47^{phox}$ PAB^{short} (Fig. 6*B*, lane 6).

To our surprise, neither $p47^{phox}$ AB (Fig. 6*C*) nor PAB^{short} (Fig. 6*D*) had any discernable impact on WRC activity. First, they did not enhance WRC activity in the basal state (without Rac1 activation, blue lines in Fig. 6, *C* and *D*). As some WRC ligands, such as WRC-interacting receptor sequence–containing receptors, do not directly enhance WRC activity but can modulate its activity when WRC is activated by Rac1 (22), we tested whether $p47^{phox}$ exhibited a similar behavior. However, $p47^{phox}$ did not alter the activity level of WRC, whether WRC was mildly activated by an intermediate concentration of Rac1 (green lines in Fig. 6, *C* and *D*) or fully activated by a saturating concentration of Rac1 (red lines in Fig. 6, *C* and *D*).

Certain WRC ligands can have dual and opposing effects in WRC-mediated actin polymerization assays (15). For example, the dendrite branching receptor HPO-30 can promote WRC activation while simultaneously inhibiting actin polymerization, leading to potentially complex outcomes (41). However, we ruled out the possibility that the lack of effect on WRC activity was due to a similar counteracting effect of $p47^{phox}$ based on two observations. First, $p47^{phox}$ did not affect actin polymerization mediated by free WCA peptide, to which $p47^{phox}$ does not bind (Fig. 6*E*), thus eliminating potential inhibitory effect of $p47^{phox}$ on actin polymerization. Second, $p47^{phox}$ did not affect the activity of a constitutively active WRC in the absence of Rac1, thus eliminating potential complications arising from $p47^{phox}$ affecting Rac1 binding to WRC (Fig. 6*F*). Together, the data suggest that $p47^{phox}$ binding to WAVE1 86 to 230 sequence does not directly impact WRC activation.

Discussion

The crosstalk between actin remodeling and redox regulation is essential to various cellular processes. A common mechanism underlying this crosstalk involves the oxidation of actin or actin regulators, such as the oxidation of actin filaments by MICAL or various proteins by ROS molecules (9–12, 42). However, direct interactions between actin regulators and ROS production enzymes have remained elusive. The identification of the interaction between WAVE1 and $p47^{phox}$ 2 decades ago led to an intriguing model, suggesting that activated $p47^{phox}$ could simultaneously bind to $p22^{phox}$ and WAVE1, thereby potentially bridging the WRC and NOX2 into a large signalosome that coordinates actin polymerization and ROS-mediated oxidation (13, 35). In our study, we used well-characterized recombinant materials to elucidate the interaction mechanism and arrived at conclusions that differ from the earlier model.

First, we have established that $p22^{phox}$ and WRC bind to the same pocket in $p47^{phox}$, and their interactions occur in a mutually exclusive manner, rather than simultaneously. Previous studies suggesting simultaneous binding of WAVE1 and $p22^{phox}$ to $p47^{phox}$ were primarily based on yeast two-hybrid analysis and binding assays using *in vitro* translated materials (13). These studies indicated that mutating the conserved residue, W193R, within the $p22^{phox}$-binding pocket did not affect WAVE1 binding. In addition, individual SH3 domains could bind WAVE1. This was distinct from $p22^{phox}$, which requires both SH3 domains for binding (13). Our studies confirmed a direct interaction between WAVE1 and $p47^{phox}$ and further revealed multiple $p47^{phox}$ binding sequences within the WAVE1 and Abi2 subunits of the WRC.

However, in contrast to previous studies, we find that all interactions between WRC and $p47^{phox}$, regardless of the specific binding sequences involved, are mediated by the same

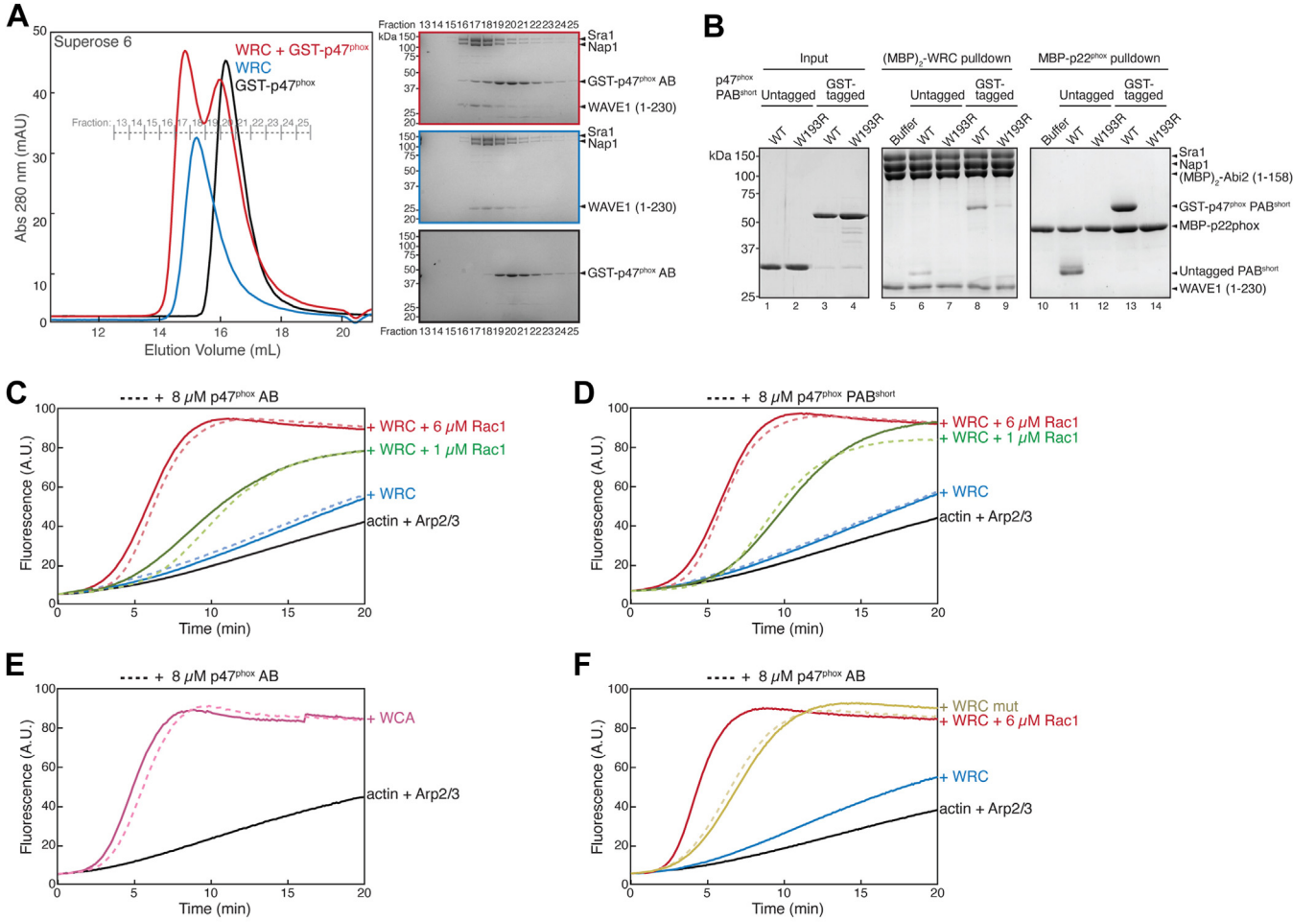

Figure 6. p47^{phox} binding does not impact WRC activity. *A*, cogel filtration of WRC$^{\Delta 230}$ with glutathione-*S*-transferase (GST)-p47^{phox} AB, showing chromatograms of indicated samples on *left* and *Coomassie blue–stained* SDS-PAGE gels on *right*. Gel images are aligned *vertically* over indicated fractions. The formation of a WRC–p47^{phox} complex is indicated by the shift of the WRC peak from fraction 18 to 17 and the appearance of p47^{phox} in fractions 16 to 18. *B*, *Coomassie blue–stained* SDS-PAGE gels of amylose beads pull down using indicated MBP-tagged baits (41), comparing untagged *versus* GST-tagged p47^{phox} PAB^{short}. *C–F*, pyrene-actin polymerization assay at indicated conditions. Reactions contain 3 to 4 μM actin (5% pyrene-labeled), 10 nM Arp2/3, 0.1 μM WRC^{230WCA} or WCA, and indicated Rac1^{Q61L} and/or p47^{phox}. WCA, WH2-central-acidic; WRC, WAVE regulatory complex.

p22-^{phox}-binding pocket. These interactions share common features with p22^{phox} binding, as they are all abolished by W193R mutation, can be competitively disrupted by p22^{phox} binding, require dual SH3 domains but not individual SH3 domains and cannot occur with autoinhibited FL p47^{phox}. The discrepancy between our findings and prior results likely stems from differences in the materials involved. Over years of effort to establish recombinant WRC purification, it has become evident that individually expressed or purified WRC subunits, including WAVE1, are prone to protein aggregation, which can lead to erroneous experimental outcomes (15). Using our meticulously purified materials and rigorous controls, we have now clarified the previous observations and established that WRC and p22^{phox} bind to p47^{phox} at the same binding site and in a mutually exclusive manner.

WRC contains PRRs known to mediate interactions with various PRR-binding proteins, such as SH3-containing proteins like WRP (43)- and EVH1-containing proteins like Ena/VASP (37, 39). Since the unstructured PRR sequences are not involved in WRC assembly or autoinhibition, these interactions typically do not have a direct impact on WRC activity. Instead, they mainly influence WRC localization and its connections with other signaling pathways. Our study has expanded the list of WRC ligands by establishing p47^{phox} as a genuine WRC-binding protein. This interaction can potentially connect WRC-mediated actin polymerization with pathways involving p47^{phox}, such as NOX2 activation.

In addition to the PRR sequences in WAVE1 and Abi2 that interact with p47^{phox}, we have also uncovered noncanonical SH3-binding sequences within the region spanning residues 86 to 186 of WAVE1. This finding is consistent with the promiscuity of SH3-binding sequences (40, 44) and may prompt reevaluation of other SH3- or EVH1-containing WRC ligands to determine whether they also interact with this specific region. Notably, this region contains the meander sequence, which winds across a conserved surface on Sra1 (Fig. 5*A*), playing a key role in WRC autoinhibition and activation. Therefore, it is possible that other SH3-containing proteins may dock at this sequence to modulate WRC activity, although, unexpectedly, p47^{phox} binding to this noncanonical

sequence did not affect WRC activity under various tested conditions.

Our results propose a model distinct from previous reports. In this revised model, upon activation, $p47^{phox}$ can participate in two distinct processes in the cell (Fig. 7). In one process, $p47^{phox}$ translocates to the membrane by binding to $p22^{phox}$ and, together with other NOX2 subunits, assembles into an active NOX2 complex to initiate ROS production. In another process, $p47^{phox}$ binds to membrane-associated WRC at multiple sequences. While the precise mechanisms by which the $p47^{phox}$–WRC interaction modulates actin dynamics in a cellular context remains to be elucidated, several possibilities exist. First, although $p47^{phox}$ binding to WRC does not directly control WRC activity, it could potentially regulate WRC's interactions with other SH3-binding proteins or serve as a scaffold to recruit $p47^{phox}$-binding ligands. Second, this interaction could influence WRC localization, considering that the PX domain of $p47^{phox}$ interacts with inositol phospholipids at membranes (45, 46), which are also potential activators of the WRC (19, 47). Third, $p47^{phox}$ may interact with actin either directly through its C-terminal sequence (residues 319–337) (48) or indirectly through its PX domain binding to meosin (49, 50). Intriguingly, both inositol phospholipids and Rac1 are shared factors between NOX2 assembly and WRC activation (8). Thus, the cooperative actions of Rac1 activation, inositol phospholipids production, and $p47^{phox}$ activation may play a pivotal role in orchestrating ROS production and actin polymerization (Fig. 7).

Taken together, our work clarifies the connection between WRC and $p47^{phox}$, providing a foundation for exploring the interplay between actin polymerization and ROS production in various cellular processes.

Limitations of the current study

We recognize several limitations in our study, primarily the lack of cellular experiments to elucidate the functional significance of p47phox binding to the WRC within a cellular context. For instance, it remains unknown whether p47phox binding influences WRC activity, localization, or composition inside the cells; whether NOX2 assembly and WRC binding compete for the same pool of activated p47phox; and how the activities of NOX2 and WRC are spatiotemporally linked or balanced through p47phox. We anticipate that our biochemical results, obtained from carefully characterized materials, will pave the way for future investigations into these intriguing questions.

Experimental procedures

Protein purification

Various human WRCs were expressed and purified essentially as previously described (17, 18, 23, 36). All constructs were generated by standard molecular biology procedures and verified by Sanger sequencing. To improve the yield of FL WAVE1 expression from bacterial cells, the coding sequences were synthesized from Integrated DNA Technologies using codons optimized for *Escherichia coli* expression. The coding sequence of FL human $p47^{phox}$ was obtained from GE Healthcare (IMAGE: 3633829). DNA constructs, protein sequences, and cloning primers used in this study are listed in Tables S1–S3, respectively.

Reconstitution of recombinant WRCs followed previously established protocols involving purification of individual subunits, assembly of subcomplexes (*i.e.*, Sra1/Nap1 dimer and WAVE1/Abi2/HSPC300 trimer), and final purification of the WRC pentamer by a series of affinity, ion exchange, and gel-filtration chromatography steps (23, 36). Sra1 and Nap1 were expressed in Tni cells using the ESF 921 medium (Expression Systems). Other proteins were expressed in BL21 $(DE3)^{T1R}$ cells (Sigma) at 18 °C overnight or ArcticExpress (DE3) RIL cells (Stratagene) at 10 °C for 24 h. Various WRCs used in this study behaved similarly during each step of the reconstitution, showing no sign of misassembly or aggregation.

Different GST-tagged $p47^{phox}$ constructs were purified by Glutathione Sepharose beads (Cytiva), followed by anion-exchange chromatography through a Source Q15 column and gel filtration through a Hiload Superdex 75 column. To obtain untagged $p47^{phox}$ proteins, GST-$p47^{phox}$ was treated with Tev protease overnight at 4 °C to cleave off the GST tag, followed by ion exchange and gel-filtration chromatography to obtain the untagged protein. Proteins including Arp2/3

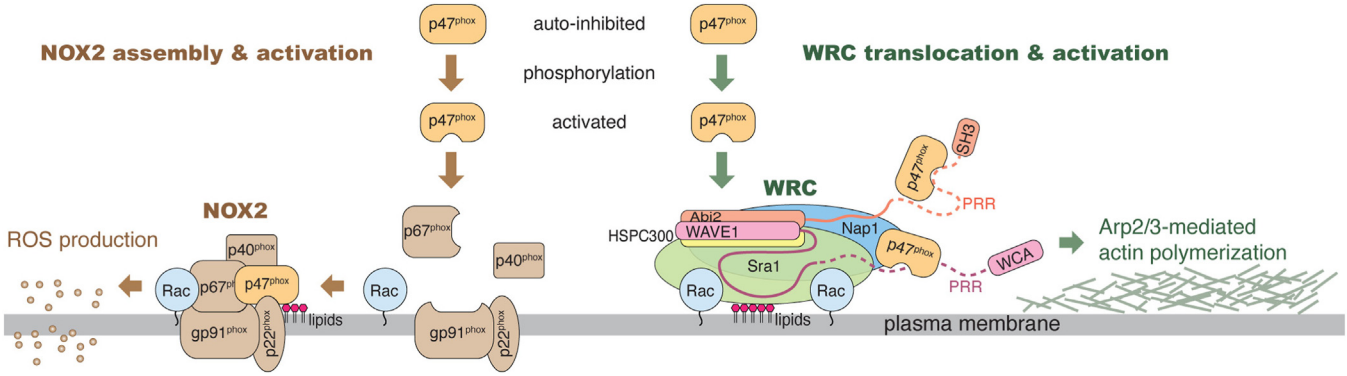

Figure 7. Schematic depicting an updated model detailing the potential involvement of activated $p47^{phox}$ in the processes of ROS production and actin cytoskeletal remodeling. This model is based on our interpretation of the biochemical data and warrants further validation through cellular experiments to fully understand its functional implications. ROS, reactive oxygen species.

complex, actin, WAVE1 WCA, TEV protease, HRV 3C protease, and untagged Rac1^{Q61L} were purified as previously described (23, 36). All ion exchange and gel-filtration chromatography steps were performed using columns from Cytiva on an ÄKTA pure protein purification system.

GST pull-down assay

GST pull-down experiments were performed as previously described (17, 23). Typically, 250 to 300 pmol of GST-tagged proteins as baits and 100 to 150 pmol of WRCs as preys were mixed with 20 μl of Glutathione Sepharose beads in 1 ml of binding buffer (10 mM Hepes pH 7, 100 mM NaCl, 5% (w/v) glycerol, 2 mM $MgCl_2$, and 5 mM β-mercaptoethanol or 1 mM DTT) at 4 °C for 30 min, followed by three washes using 1 ml of the binding buffer in each time of wash. Bound proteins were eluted with the GST elution buffer (100 mM Tris–HCl pH 8.5, 2 mM $MgCl_2$, and 30 mM reduced GSH) and examined by SDS-PAGE.

Pyrene-actin polymerization assay

Actin polymerization assays were performed as previously described with some modifications here (17, 23). Each reaction (120 μl) contained 3 to 4 μM actin (5% pyrene labeled), 10 nM Arp2/3 complex, 100 nM of WRC^{230WCA} constructs or WAVE1 WCA, and desired concentrations of untagged Rac1^{Q61L} and/or untagged p47^{phox} in the NMEH20GD buffer (50 mM NaCl, 1 mM $MgCl_2$, 1 mM EGTA, 10 mM Hepes pH 7, 20% (w/v) glycerol, and 1 mM DTT). Pyrene-actin fluorescence was recorded every 5 s at 22 °C, one reaction per measurement using single-channel pipettes to minimize air bubbles or pipetting errors, using a 96-well flat-bottom black plate (Greiner Bio-One) in a Spark plate reader (Tecan), with excitation at 365 nm and emission at 407 nm (15 nm bandwidth for both wavelengths).

Data availability

All data are contained within the manuscript. Further information and requests for resources and reagents including DNA constructs and recombinant proteins should be directed to Baoyu Chen.

Supporting information—This article contains supporting information (17, 22).

Author contributions—K. J. B. and B. C. conceptualization; K. J. B. and B. C. funding acquisition; B. C. supervision; S. V. N. P. K, B. J. S, K. J. B, and C. A. A. data curation; S. V. N. K. and B. C. writing-original draft; S. V. N. P. K., B. J. S., C. A. A., K. J. B., and B. C. visualization; S. V. N. P., B. J. S., K. J. B., and C. A. A. investigation.

Funding and additional information—The research was supported by the American Heart Association (19IPLOI34660134 [to B. C. and K. J. B.]) and the National Institutes of Health (R35 GM128786 [to B. C.]). The content is solely the responsibility of the authors and does not necessarily represent the official views of the National Institutes of Health.

Conflict of interest—The authors declare that they have no conflicts of interest with the contents of this article.

Abbreviations—The abbreviations used are: AIR, autoinhibitory region; FL, full length; GST, glutathione-*S*-transferase; ICD, intracellular domain; MBP, maltose-binding protein; PRR, proline-rich region; ROS, reactive oxygen species; SH3, Src homology 3; WCA, WH2-central-acidic; WRC, WAVE regulatory complex.

References

1. Gellert, M., Hanschmann, E. M., Lepka, K., Berndt, C., and Lillig, C. H. (2015) Redox regulation of cytoskeletal dynamics during differentiation and de-differentiation. *Biochim. Biophys. Acta Gen. Subj.* **1850**, 1575–1587
2. Schröder, K. (2014) NADPH oxidases in redox regulation of cell adhesion and migration. *Antioxid. Redox Signal.* **20**, 2043–2058
3. Hurd, T. R., DeGennaro, M., and Lehmann, R. (2012) Redox regulation of cell migration and adhesion. *Trends Cell Biol.* **22**, 107–115
4. Tochhawng, L., Deng, S., Pervaiz, S., and Yap, C. T. (2013) Redox regulation of cancer cell migration and invasion. *Mitochondrion* **13**, 246–253
5. Moldovan, L., Moldovan, N. I., Sohn, R. H., Parikh, S. A., and Goldschmidt-Clermont, P. J. (2000) Redox changes of cultured endothelial cells and actin dynamics. *Circ. Res.* **86**, 549–557
6. Stanley, A., Thompson, K., Hynes, A., Brakebusch, C., and Quondamatteo, F. (2014) NADPH oxidase complex-derived reactive oxygen species, the actin cytoskeleton, and Rho GTPases in cell migration. *Antioxid. Redox Signal.* **20**, 2026–2042
7. Xu, Q., Huff, L. P., Fujii, M., and Griendling, K. K. (2017) Redox regulation of the actin cytoskeleton and its role in the vascular system. *Free Radic. Biol. Med.* **109**, 84–107
8. Acevedo, A., and González-Billault, C. (2018) Crosstalk between Rac1-mediated actin regulation and ROS production. *Free Radic. Biol. Med.* **116**, 101–113
9. Wilson, C., Terman, J. R., González-Billault, C., and Ahmed, G. (2016) Actin filaments-A target for redox regulation. *Cytoskeleton (Hoboken)* **73**, 577–595
10. Griesser, E., Vemula, V., Mónico, A., Pérez-Sala, D., and Fedorova, M. (2021) Dynamic posttranslational modifications of cytoskeletal proteins unveil hot spots under nitroxidative stress. *Redox Biol.* **44**, 102014
11. Rouyère, C., Serrano, T., Frémont, S., and Echard, A. (2022) Oxidation and reduction of actin: origin, impact *in vitro* and functional consequences *in vivo*. *Eur. J. Cell Biol.* **101**, 151249
12. Balta, E., Kramer, J., and Samstag, Y. (2021) Redox regulation of the actin cytoskeleton in cell migration and adhesion: on the way to a spatiotemporal view. *Front. Cell Dev. Biol.* **8**, 618261
13. Wu, R. F., Gu, Y., Xu, Y. C., Nwariaku, F. E., and Terada, L. S. (2003) Vascular endothelial growth factor causes translocation of p47phoxto membrane ruffles through WAVE1. *J. Biol. Chem.* **278**, 36830–36840
14. Park, S. J., Kim, Y. T., and Jeon, Y. J. (2012) Antioxidant dieckol down-regulates the Rac1/ROS signaling pathway and inhibits Wiskott-Aldrich syndrome protein (WASP)-family verprolin-homologous protein 2 (WAVE2)-mediated invasive migration of B16 mouse melanoma cells. *Mol. Cells* **33**, 363–369
15. Rottner, K., Stradal, T. E. B., and Chen, B. (2021) WAVE regulatory complex. *Curr. Biol.* **31**, R512–R517
16. Kramer, D. A., Piper, H. K., and Chen, B. (2022) WASP family proteins: molecular mechanisms and implications in human disease. *Eur. J. Cell Biol.* **101**, 151244
17. Ding, B., Yang, S., Schaks, M., Liu, Y., Brown, A. J., Rottner, K., *et al.* (2022) Structures reveal a key mechanism of WAVE regulatory complex activation by Rac1 GTPase. *Nat. Commun.* **13**, 5444
18. Yang, S., Tang, Y., Liu, Y., Brown, A. J., Schaks, M., Ding, B., *et al.* (2022) Arf GTPase activates the WAVE regulatory complex through a distinct binding site. *Sci. Adv.* **8**, eadd1412
19. Lebensohn, A. M., and Kirschner, M. W. (2009) Activation of the WAVE complex by coincident signals controls actin assembly. *Mol. Cell* **36**, 512

20. Chen, Z., Borek, D., Padrick, S. B., Gomez, T. S., Metlagel, Z., Ismail, A. M., *et al.* (2010) Structure and control of the actin regulatory WAVE complex. *Nature* **468**, 533–538
21. Koronakis, V., Hume, P. J., Humphreys, D., Liu, T., Hørning, O., Jensen, O. N., *et al.* (2011) WAVE regulatory complex activation by cooperating GTPases Arf and Rac1. *Proc. Natl. Acad. Sci. U. S. A.* **108**, 14449–14454
22. Chen, B., Brinkmann, K., Chen, Z., Pak, C. W., Liao, Y., Shi, S., *et al.* (2014) The WAVE regulatory complex links diverse receptors to the actin cytoskeleton. *Cell* **156**, 195–207
23. Chen, B., Chou, H.-T. T., Brautigam, C. A., Xing, W., Yang, S., Henry, L., *et al.* (2017) Rac1 GTPase activates the WAVE regulatory complex through two distinct binding sites. *Elife* **6**, e29795
24. Brandes, R. P., and Kreuzer, J. (2005) Vascular NADPH oxidases: molecular mechanisms of activation. *Cardiovasc. Res.* **65**, 16–27
25. Lassègue, B., San Martín, A., and Griendling, K. K. (2012) Biochemistry, physiology, and pathophysiology of NADPH oxidases in the cardiovascular system. *Circ. Res.* **110**, 1364–1390
26. El-Benna, J., Dang, P. M. C., Gougerot-Pocidalo, M. A., Marie, J. C., and Braut-Boucher, F. (2009) p47phox, the phagocyte NADPH oxidase/NOX2 organizer: structure, phosphorylation and implication in diseases. *Exp. Mol. Med.* **41**, 217–225
27. Bedard, K., and Krause, K.-H. (2007) The NOX family of ROS-generating NADPH oxidases: physiology and pathophysiology. *Physiol. Rev.* **87**, 245–313
28. Magnani, F., and Mattevi, A. (2019) Structure and mechanisms of ROS generation by NADPH oxidases. *Curr. Opin. Struct. Biol.* **59**, 91–97
29. Nocella, C., D'Amico, A., Cammisotto, V., Bartimoccia, S., Castellani, V., Loffredo, L., *et al.* (2023) Structure, activation, and regulation of NOX2: at the crossroad between the innate immunity and oxidative stress-mediated pathologies. *Antioxidants (Basel)* **12**, 429
30. Liu, R., Song, K., Wu, J. X., Geng, X. P., Zheng, L., Gao, X., *et al.* (2022) Structure of human phagocyte NADPH oxidase in the resting state. *Elife* **11**, e83743
31. Groemping, Y., Lapouge, K., Smerdon, S. J., and Rittinger, K. (2003) Molecular basis of phosphorylation-induced activation of the NADPH oxidase. *Cell* **113**, 343–355
32. Yuzawa, S., Suzuki, N. N., Fujioka, Y., Ogura, K., Sumimoto, H., and Inagaki, F. (2004) A molecular mechanism for autoinhibition of the tandem SH3 domains of p47phox, the regulatory subunit of the phagocyte NADPH oxidase. *Genes Cells* **9**, 443–456
33. Noreng, S., Ota, N., Sun, Y., Ho, H., Johnson, M., Arthur, C. P., *et al.* (2022) Structure of the core human NADPH oxidase NOX2. *Nat. Commun.* **13**, 6079
34. Ogura, K., Nobuhisa, I., Yuzawa, S., Takeya, R., Torikai, S., Saikawa, K., *et al.* (2006) NMR solution structure of the tandem Src homology 3 domains of p47 phox complexed with a p22phox-derived proline-rich peptide. *J. Biol. Chem.* **281**, 3660–3668
35. Ushio-Fukai, M. (2006) Localizing NADPH oxidase-derived ROS. *Sci. STKE* **2006**, re8
36. Chen, B., Padrick, S. B., Henry, L., and Rosen, M. K. (2014) Biochemical reconstitution of the WAVE regulatory complex. *Methods Enzymol.* **540**, 55–72
37. Chen, X. J., Squarr, A. J., Stephan, R., Chen, B., Higgins, T. E., Barry, D. J., *et al.* (2014) Ena/VASP proteins cooperate with the WAVE complex to regulate the actin cytoskeleton. *Dev. Cell* **30**, 569–584
38. Ismail, A. M., Padrick, S. B., Chen, B., Umetani, J., and Rosen, M. K. (2009) The WAVE regulatory complex is inhibited. *Nat. Struct. Mol. Biol.* **16**, 561–563
39. Shi, R., Kramer, D. A., Chen, B., and Shen, K. (2021) A two-step actin polymerization mechanism drives dendrite branching. *Neural Dev.* **16**, 3
40. Teyra, J., Huang, H., Jain, S., Guan, X., Dong, A., Liu, Y., *et al.* (2017) Comprehensive analysis of the human SH3 domain family reveals a wide variety of non-canonical specificities. *Structure* **25**, 1598–1610.e3
41. Kramer, D. A., Narvaez-Ortiz, H. Y., Patel, U., Shi, R., Shen, K., Nolen, B. J., *et al.* (2023) The intrinsically disordered cytoplasmic tail of a dendrite branching receptor uses two distinct mechanisms to regulate the actin cytoskeleton. *Elife* **12**, e88492
42. Rajan, S., Terman, J. R., and Reisler, E. (2023) MICAL-mediated oxidation of actin and its effects on cytoskeletal and cellular dynamics. *Front. Cell Dev. Biol.* **11**, 1124202
43. Soderling, S. H., Binns, K. L., Wayman, G. A., Davee, S. M., Ong, S. H., Pawson, T., *et al.* (2002) The WRP component of the WAVE-1 complex attenuates Rac-mediated signalling. *Nat. Cell Biol.* **4**, 970–975
44. Saksela, K., and Permi, P. (2012) SH3 domain ligand binding: what's the consensus and where's the specificity? *FEBS Lett.* **586**, 2609–2614
45. Kanai, F., Liu, H., Field, S. J., Akbary, H., Matsuo, T., Brown, G. E., *et al.* (2001) The PX domains of p47phox and p40phox bind to lipid products of PI(3)K. *Nat. Cell Biol.* **3**, 675–678
46. Karathanassis, D., Stahelin, R. V., Bravo, J., Perisic, O., Pacold, C. M., Cho, W., *et al.* (2002) Binding of the PX domain of p47(phox) to phosphatidylinositol 3,4-bisphosphate and phosphatidic acid is masked by an intramolecular interaction. *EMBO J.* **21**, 5057–5068
47. Oikawa, T., Yamaguchi, H., Itoh, T., Kato, M., Ijuin, T., Yamazaki, D., *et al.* (2004) PtdIns(3,4,5)P3 binding is necessary for WAVE2-induced formation of lamellipodia. *Nat. Cell Biol.* **6**, 420–426
48. Tamura, M., Itoh, K., Akita, H., Takano, K., and Oku, S. (2006) Identification of an actin-binding site in p47phox an organizer protein of NADPH oxidase. *FEBS Lett.* **580**, 261–267
49. Zhan, Y., He, D., Newburger, P. E., and Zhou, G. W. (2004) p47phox PX domain of NADPH oxidase targets cell membrane via moesin-mediated association with the actin cytoskeleton. *J. Cell Biochem.* **92**, 795–809
50. Wientjes, F. B., Reeves, E. P., Soskic, V., Furthmayr, H., and Segal, A. W. (2001) The NADPH oxidase components p47(phox) and p40(phox) bind to moesin through their PX domain. *Biochem. Biophys. Res. Commun.* **289**, 382–388